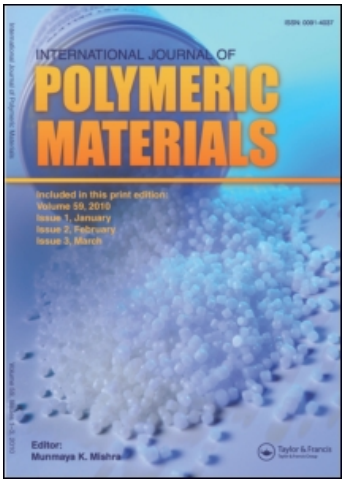

International Journal of Polymeric Materials
Publication details, including instructions for authors and subscription information:
http://www.informaworld.com/smpp/title~content=t713647664

Boundary Layers and Physico-Mechanical Properties of Adhesive Joints: Part II Theoretical Model

R. A. Turusov[a]; A. S. Freidin[b]; V. N. Kestelman[c]
[a] Institute of Chemical Physics, Moscow, Russia [b] Central Institute of Building Constructions, Moscow, Russia [c] JBK International, Radnor, PA, USA

To cite this Article Turusov, R. A. , Freidin, A. S. and Kestelman, V. N.(1995) 'Boundary Layers and Physico-Mechanical Properties of Adhesive Joints: Part II Theoretical Model', International Journal of Polymeric Materials, 29: 1, 43 — 59
To link to this Article: DOI: 10.1080/00914039508009678
URL: http://dx.doi.org/10.1080/00914039508009678

Intern. J. Polymeric Mater., 1995, Vol. 29, pp. 43–59
Reprints available directly from the publisher
Photocopying permitted by license only

Boundary Layers and Physico-Mechanical Properties of Adhesive Joints: Part II Theoretical Model

R. A. TURUSOV

Institute of Chemical Physics, Kosygin Str. 4, Moscow, 117997, Russia

and

A. S. FREIDIN

Central Institute of Building Constructions, Institutskaya Str. 6, Moscow 109389, Russia

and

V. N. KESTELMAN*

JBK International, Radnor, PA 19087, USA

(Received April 4, 1994; in final form October 25, 1994)

A calculating method is presented that takes into consideration the formation of a boundary layer at the interface between the adhesive and substrate. The structure and properties of this layer differ from those of the adhesive and the substrate. The method is applied to predict the performance of the adhesive lap shear joint and the results of the model are compared with the experimental data.

KEY WORDS Adhesives, shear strength, lap joint, theoretical model, boundary layer model.

INTRODUCTION

In a previous study,[1] we presented evidence that the adhesives (paints, coatings, etc.) develop boundary layers whose structure and properties differ from the structure and properties of the rest of the adhesives. It has also been shown that many effects contribute to the formulation of the boundary layer, which, in turn, has a significant effect on the performance of the adhesive joint. In this article, we describe an attempt to analyze and predict the adhesive joint performance by means

*To whom all inquiries should be addressed. P.O. Box 8303, Radnor, PA 19087.

of a mathematical model that takes into consideration the existence of a boundary layer.

BOUNDARY LAYER CALCULATING METHOD

In the calculations, we assume that there is an intermediate layer of undefined thickness and properties which are different from those of the adhesive and substrate.

The principles and the results of this "boundary method" will be presented for the "lap joint" used to determine the shear strength of the joint.

Let us consider one-dimensional model of composite or adhesive joint consisting of $m + 1 = 1 + n/2$ of glued plates (bars) with the height $h_0, h_2, \ldots, h_{2m}$, of m adhesive layers with the height $h_1, h_3, \ldots, h_{2m-1}$ and of n boundary layers $h_1^*, h_2^*, \ldots, h_n^*$.

Outer forces P are applied to end faces of edge bars 0 and m (see Figure 1). In

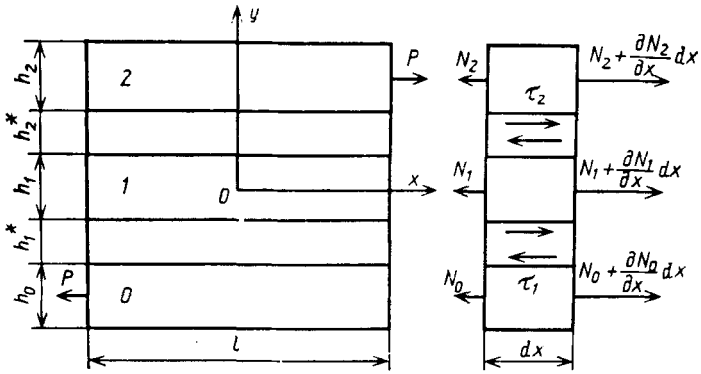

FIGURE 1 Fragment of multi-layer plate with acting inner forces and stresses (one-dimensional problem).

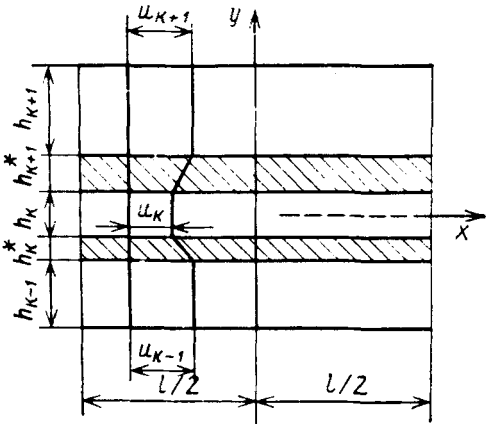

FIGURE 2 Shifts in system elements.

such one-dimensional model the probable stress change over the height of each layer is not considered. It is assumed, that stresses within any layer are uniformly distributed over its height and they depend only on longitudinal "x" coordinate. In a one-dimensional treatment only tangential stresses $\tau_1, \tau_2, \ldots, \tau_n$ are considered in boundary layers (Figure 1). Boundary layer medium is modelled by a certain anysotropic medium, Young's modulus of which in X direction tends to $0 E_{xx} \to 0$. Such medium can be visualized as a set of thin, elastic, short small bars, perpendicular to boundary surface and not touching one another. Such medium can also experience normal stresses σ_y, but in this one-dimensional shear analysis they can be disregarded.

Consider the general case of glued substrates and adhesive layers. There, simultaneously with elastic deformations l_k additional deformations can develop such as: reversible viscous-elastic deformations ε_k^*, irreversible or plastic deformations ε_k^0, temperature strain ε_{tk}, shrinking deformations ε_{ck} (as result of phase transformation or chemical reaction), humidity deformations ε_{hk} etc. If these deformations are small, the full deformation can be presented in the form of the sum of all the deformations mentioned.

Here we do not take into consideration the deformations ε_k^* and ε_k^0, and the only elastic deformations in boundary layers will be always taken into account. In addition, we will limit the considerations to uniform distribution of temperature and moisture content in layers.

For temperature and humidity deformations we will use the known simple relationships

$$\varepsilon_{tk} = \alpha_{tk} \cdot \Delta T, \quad \varepsilon_{hk} = \alpha_{hk} \cdot \Delta W \tag{1}$$

and a summarizing deformation ε_{qk} will be introduced, equal either to ε_{tk}, or to ε_{hk}, or to their sum ($k = 0, 1, 2, \ldots, n = 2m$).

In Figure 1, in the right part, the fragment of multilayer structure is presented, with length dx and with inner forces, acting in it, which are taken into consideration in one-dimensional problem.

The condition of element balance dx of one-dimensional bar "k" with width of ($k = 0, 1, 2, \ldots, n$) is the equality to zero of projections of all the forces, acting upon axis x:

$$-\tau_k b\, dx - N_k b + \tau_{k+1} b\, dx + [N_k + (dN_k/dx)\, dx] = 0$$

Hence we obtain differential equation of element equilibrium of "k" bar:

$$\tau_k - \tau_{k+1} = dN_k/dx \quad k = 0, 1, 2, \ldots, \tag{2}$$

In (2) $N_k = \sigma_{xk} h_k$ is the force, acting upon the unity of model width, σ_{xk} = normal stress. If tangential stresses are not applied to outer bar surfaces 0 and n, $\tau_0 = \tau_{n+1} = 0$.

The full deformation of "k" bar along x-axis consists of the elastic deformation l_k and the summarized one ε_{qk}:

$$\varepsilon_{xk} = e_k + \varepsilon_{qk} = N_k/(h_k E_k) + \varepsilon_{qk} \tag{3}$$

It is connected by Koschi relationship with U_k shift along the x-axis:

$$\varepsilon_{xk} = dU_k/dx \tag{4}$$

However, the V_k shifts in all the layers in direction of y-axis can be considered only as a function of y, i.e. $V_k = V_k(y)$.

As the thickness of boundary layer, performing the shear, is small it can be considered, that U_k dependence on thickness follows a linear law:

$$U_k^* = a_k + b_k y \sum_{i=0}^{k-1} (h_i + h_i^*) \le y \le \sum_{i=0}^{k-1} (h_i + h_i^*) + h_k^*;$$

$$h_0^* = 0, \quad k = 0, 1, \ldots, n \tag{5}$$

$$a_k = \frac{(S_{k-1} + h_k^*)U_{k-1} + S_{k-1}U_k}{h_k^*}; \quad b_k = \frac{U_k - U_{k-1}}{h_k^*}; \quad S_{k-1} = \sum_{i=0}^{k-1} (h_i + h_i^*) \tag{6}$$

Since $V_k^* = V_k^*(y)$, the shear deformations in boundary layer, are:

$$\varepsilon_{xy,k} = \partial U_k/\partial y + \partial V_k/\partial x = dU_k/dy \tag{7}$$

From (5)–(7) we obtain:

$$\varepsilon_{xy,k} = (U_k - U_{k-1})/h_k^* \tag{8}$$

Shear deformations of elastic boundary layer are related to shear stresses τ_k by means of Hooke's law:

$$\varepsilon_{xy,k} = e_{xy,k} = \tau_k/G_k \tag{9}$$

From (3), (4), (8) and (9) we obtain:

$$d\tau_k/dx = (G_k/h_k^*)[N_k/(E_k h_k) - N_{k-1}(E_{k-1}h_{k-1}) + \varepsilon_{qk} - \varepsilon_{q,k-1}] \tag{10}$$

Differentiating (2) and excluding derivatives of tangential stresses by means of (10), we obtain system of equations for unknown functions $N_k(x)$:

$$\frac{d^2N_k}{dx^2} - \left(\frac{G_k}{h_k^* h_k E_k} + \frac{G_{k+1}}{h_{k+1}^* h_k E_k}\right) N_k + \frac{G_k}{h_k^* h_{k-1} G_{k-1}} N_{k-1} + \frac{G_{k+1}}{h_{k+1}^* h_{k+1} E_{k+1}} N_{k+1}$$

$$+ \frac{G_{k+1}}{h_{k+1}^*}(\varepsilon_{q,k+1} - \varepsilon_{q,k}) - \frac{G_k}{h_k^*}(\varepsilon_{qk} - \varepsilon_{q,k-1}) = 0 \tag{11}$$

For layers 0 and n we obtain, respectively:

$$d^2N_0/dx^2 - (G_1/h_1^*)[N_0/(h_0E_0) - N_1/(h_1E_1) - \varepsilon_{q1} + \varepsilon_{q0}] = 0$$
$$d^2N_n/dx^2 - (G_n/h_n^*)[N_n/h_nE_n) - N_{n-1}/(h_{n-1}E_{n-1}) + \varepsilon_{qn} - \varepsilon_{qn-1}] = 0 \quad (12)$$

Systems (11) and (12) contains $n + 1$ equation for finding $n + 1$ of unknown N_k. The computational solution of this system does not present principal difficulties. For particular case $n + 1$ of similar layers and n of boundary layers the solution is obtained in closed form as a superposition of exponents.

In Figures 3a,b and 4a,b as an example, distribution curves of relative normal stresses are given in plates 0, 1, 2 and of tangential stresses—in boundary layers 1, 2 from the action only of shear forces P (see Figure 1) (Figure 3), and only from the action of temperature (Figure 4). It is the model of hybrid composite material, consisting of mono-layer of organic high-modulus fibres (brand SVM, analog to

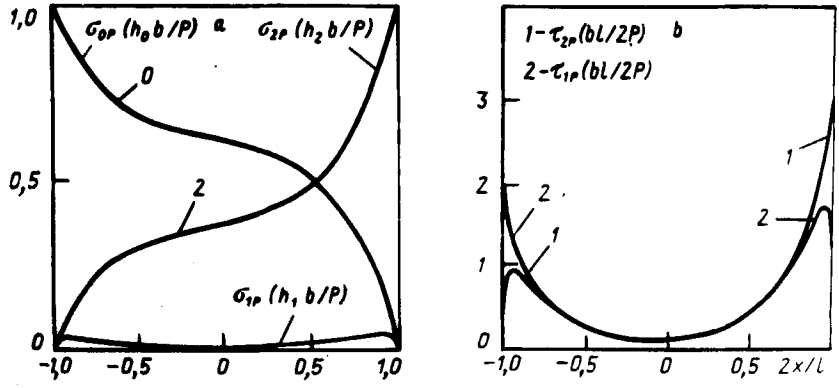

FIGURE 3 Distribution of normal (a) and tangential (b) stresses in the model of hybride composite material under the influence of shear forces.

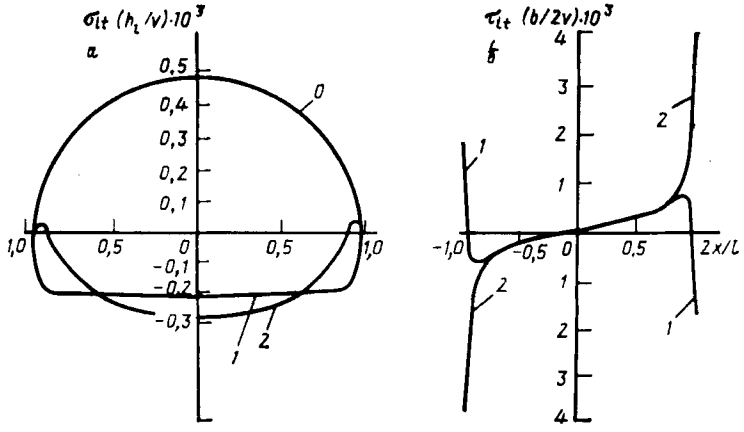

FIGURE 4 Distribution of normal temperature stresses (a) in substrate plates 0 and 2 and in adhesive layer 1, as well as of tangential temperature stresses in boundary layers h_1^* (1) and h_2^* (2); (b) $V = T - T_0$.

USA-made Kevlar fibres, but with fibrillar structure)—layer 0; of mono-layer of glass fibres-layer 2; and of connecting layer of epoxy composition—layer 1. In the calculations, it was assumed that the boundary layer properties were identical. Calculations were carried out using the following geometrical and physical parameters of the model:

$$SVM{:}E_0 = 1.2 \cdot 10^5 \text{ MPa}, \; h_0 = 0.01 \text{ mm}; \quad \alpha_{t0} = 0$$

glass fibre:

$$E_a = 0.7 \cdot 10^5 \text{ MPa}, \; h_2 = 0.01 \text{ mm}; \quad \alpha_{t2} = 8 \cdot 10^{-6} \; 1/k$$

epoxy resin:

$$E_1 = 3 \cdot 10^3 \text{ MPa}, \; h_1 = 0.009 \text{ mm}; \quad \alpha_{t1} = 8 \cdot 10^{-5} \; 1/k;$$

$$g = h_1^*/G_1 = h_2^*/G_2 = h^*/G = 10^4 \text{ MPa/mm}; \quad l = 20 \text{ mm}, \quad b = 1 \text{ mm}$$

(b = width of specimen).

The calculations show that normal tensile stresses σ_{1P} in Figure 3a have in the middle layer two maxima near end faces. The presence of similar, but more strongly developed maxima, is found also in the solution of two-dimensional problem of a simple reinforced polymer. In this case, the reinforcing element represents the middle layer 1, and at its surface (layers 0 and 2) there is the polymer matrix. The existence of such maxima determines also the place of failure in this layer (or fiber).

Regarding the temperature related stresses it should be noted that the two substrate layers (0 and 1) and the adhesive layer (1) contribute to their formation. The corresponding stress distribution, shown in Figure 4, is rather unusual and unexpected. For example, the distribution of tangential stresses in the boundary layer 1 (see Figure 4) changes its sign near the end faces, and the normal stresses in substrate 2 are everywhere compressive except near the end faces where they become tensile.

In the solution of the problem considered, the tangential stresses in boundary layers 1 and 2 in corner points near end face at $x = \pm l/2 (\zeta = 2x/l = \pm 1)$ are not equal to zero, although no tangential stresses are applied from the outside. This is the consequence of the one-dimensional approximation. The accurate account of boundary conditions is possible only by means of two-dimensional problem.

SHEAR IN LAP JOINT

Turning to consideration of design and tests of plate lap joint, the scheme of which is shown in Figure 5, we note that it is widely used for the determination of shear adhesive strength by glueing metal, wood, ceramic and other plates (USSR: GOST 14759-69; USA: ASTMD 1002-64T, MIL-A-5090D, MIL-A-140X etc.). In this case

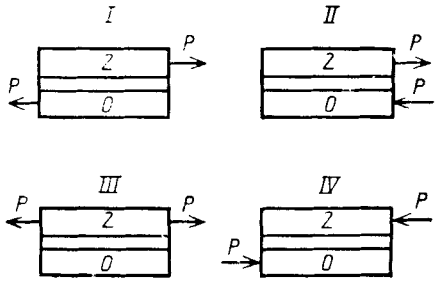

FIGURE 5 Variants of loading for plate lap joint.

the bars usually glued together 0 and 2 are identical. Therefore, in the formulas, of the previous section, given above, it should be taken:

$$E_0 = E_2; \quad h_0 = h_2; \quad \varepsilon_{q0} = \varepsilon_{q2}; \quad \alpha_{t0} = \alpha_{t2}; \quad G_1/h_1^* = G_2/h_2^* = G/h^* = g$$

In this case, Equations (11) and (12) for loading variants I, III, IV (see Figure 5) will obtain the following form:

$$\begin{aligned} d^2N_0/dx^2 + g(-k_0N_0 + k_1N_1 + \varepsilon_{g1} - \varepsilon_{g0}) &= 0 \\ d^2N_2/dx^2 + g(-k_0N_2 + k_1N_1 + \varepsilon_{g1} - \varepsilon_{g0}) &= 0 \qquad (12') \\ N_0 + N_1 + N_2 &= P/b \end{aligned}$$

For variant II, the last equation has the form of $N_0 + N_1 + N_2 = 0$, for variant IV, the P value changes for $-P$.

Let us substitute N_1 from $(12')_3$ into the first two equations, and then these equations will be summed up and subtracted. This leads to

$$\varphi'' - (k_0 + 2k_1)g\varphi + 2gK_1P/b + 2g(\varepsilon_{q1} - \varepsilon_{q0}) = 0; \quad f'' - gk_0f = 0 \qquad (13)$$

$$\varphi = N_0 + N_2; \quad f = N_0 - N_2; \quad k_0 = 1/E_0h_0; \quad k_1 = 1/E_1h_1 \qquad (14)$$

For variant II the first equation in (13) doesn't contain member with P/.

The particular solution of inhomogeneous Equation (13) is as follows:

$$\varphi_\tau = 2(k_1P/b + \varepsilon_{q1} - \varepsilon_{q0})/(k_0 + 2k_1) \qquad (15)$$

The solutions of system (13) assumes the form:

$$\varphi = A_1 \operatorname{sh} W_1x + B_1 \operatorname{ch} W_1x + \varphi_\tau; \quad f = A_2 \operatorname{sh} W_2x + B_2 \operatorname{ch} W_2x. \qquad (16)$$

We limit ourselves to the consideration of loading variant I, namely the shear of glued plates by means of tensile forces.

In this case, the boundary conditions are:

$$\begin{aligned} &x = l/2\text{: } N_0 = 0,\ N_1 = 0,\ N_2 = P/b;\quad \varphi = P/b,\ f = -P/b;\\ &x = -l/2\text{: } N_0 = P/b,\ N_1 = 0,\ N_2 = 0;\quad \varphi = P/b,\ f = P/b \end{aligned} \tag{17}$$

The solution of system (13):

$$\begin{aligned} &\varphi = (P/b - \varphi_\tau)(\operatorname{ch} W_1 x/\operatorname{ch} V_1) + \varphi_\tau;\quad f = (P/b)(\operatorname{sh} W_2 x/\operatorname{sh} V_2);\\ &W_1^2 = (k_0 + 2k_1)g;\quad W_2^2 = k_0 g;\quad V_1 = W_1 l/2;\ V_2 = W_2 l/2 \end{aligned} \tag{18}$$

We present the final solutions for forces and stresses in the form of two types of residual stresses, those influenced by shrinkage and temperature and those created by applied outer forces P.

$$\begin{aligned} N_0(x) &= \sigma_0 h_0 = \frac{\varphi + f}{2} = \frac{p}{2b}\left(\frac{k_0}{k_0 + 2k_1}\cdot\frac{\operatorname{ch} W_1 x}{\operatorname{ch} V_1} - \frac{\operatorname{sh} W_2 x}{\operatorname{sh} V_2} + \frac{2k_1}{k_0 + 2k_1}\right) + \frac{\varphi_T}{2}\\ N_2(x) &= \sigma_2 h_0 = \frac{\varphi - f}{2} = \frac{p}{2b}\left(\frac{k_0}{k_0 + 2k_1}\frac{\operatorname{ch} W_1 x}{\operatorname{ch} V_1} + \frac{\operatorname{sh} W_2 x}{\operatorname{sh} V_2} + \frac{2k_1}{k_0 + 2k_1}\right) + \frac{\varphi_T}{2}\\ N_1(x) &= \sigma_1 h_1 = \frac{p}{b} - (N_0 + N_2) = \frac{p}{b}\frac{k_0}{k_0 + 2k_1}\left(1 - \frac{\operatorname{ch} W_1 x}{\operatorname{ch} V_1}\right) - \varphi_T\\ \tau_1(x) &= -\frac{dN_0}{dx} = \frac{P}{2b}\left(-W_1\frac{k_0}{k_0 + 2k_1}\cdot\frac{\operatorname{sh} W_1 x}{\operatorname{ch} V_1} + W_2\frac{\operatorname{ch} W_2 x}{\operatorname{sh} V_2}\right) + \tau_T\\ \tau_2(x) &= dN_2/dx = \tau_1(-x);\quad \varphi_T = \frac{2(\varepsilon_{q1} - \varepsilon_{q0})}{k_0 + 2k_1}\left(1 - \frac{\operatorname{ch} W_1 x}{\operatorname{ch} V_1}\right)\\ \tau_T &= (d\varphi/dx)/2 = \frac{W_1(\varepsilon_{q1} - \varepsilon_{q0})\operatorname{sh} W_1 x}{(k_0 + 2k_1)\operatorname{ch} V_1} \end{aligned} \tag{19}$$

In Figure 6 we present the example of distribution of tangential stresses in boundary layers, for a lap joint. In the calculations we used the following values for parameters: $g = 29600$ MPa, $l = 20$ mm, $E_0 = 2\cdot 10^4$ MPa, $E_1 = 6\cdot 10^3$ MPa, $h_0 = h_2 = 2$ mm, $h_1 = 0.2$ mm, $\alpha_1 = 8\cdot 10^{-5}\ 1/k$; $\alpha_0 = 1\cdot 10^{-5}\ 1/k$; $\Delta T = \vartheta = -100k$; $p/2b = 59\ H/\text{mm}$.

Let us consider one of the most often encountered cases: adhesive hardening is carried out at high temperature. The stresses, which appear on hardening will be disregarded. Model tests are carried out at normal temperature in shear condition by tension. It means that $\vartheta = \Delta T = T - T_0 < 0$, and $P > 0$. Usually, polymer adhesive has coefficient of linear expansion, which is higher, than that of the substrate, i.e. $\alpha_1 > \alpha_0$ and therefore $(\alpha_1 - \alpha_0)$. $\vartheta < 0$.

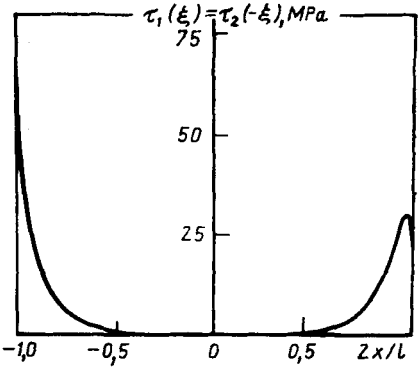

FIGURE 6 Distribution example of tangential stresses (formula 19) in lap joint.

We put down $\tau_1(\varkappa)(\ )$, taking into consideration only temperature stresses:

$$\tau_1(\varkappa) = \tau_{1p}(\varkappa) + \tau_{1T}(\varkappa) = \frac{p}{2b}\left[-\frac{W_1 k_0}{k_0 + 2k_1}\frac{\operatorname{sh} W_1 x}{\operatorname{ch} V_1} + W_2\frac{\operatorname{ch} W_2\varkappa}{\operatorname{sh} V_2}\right]$$

$$+ (\alpha_1 - \alpha_0)\,\vartheta\cdot\frac{W_1}{k_0 + 2k_1}\frac{\operatorname{sh} W_1\varkappa}{\operatorname{ch} V_1} \quad (-l/2 \le \varkappa \le l/2) \qquad (20)$$

To compare the solution (20) with experimental data of average adhesive strength, as a function of various experimental parameters, it is necessary to make certain analysis and transformation of the solution (20).

The second item in square brackets (20) is positive for all values of X, the first one is positive only for $\varkappa < 0$. The temperature member is also positive for $\varkappa < 0$. This means that $\tau_1(\varkappa)$ reaches maximum value at $\varkappa = -l/2$, and $\tau_2(\varkappa) = \tau_1(-\varkappa)$— at $\varkappa = l/2$, i.e. where tensile forces P are applied. An example of tangential stress distribution $\tau_1(\varkappa)$ is presented in Figure 6.

Now we postulate that model failure by shear takes place at the moment, when maximum value $\tau_1(\varkappa)$ reaches a certain critical vlue (τ_{ad}), which will be called the shear strength of adhesive bond of a given adhesive-substrate pair. However, experimentally we determine the integral characteristics of the model, namely the average tangential stress. This stress equals the relation between the breaking load P_b and glueing area

$$\bar{\tau} = \tau_{\min} = P_b/bl \qquad (21)$$

By means of (20) we shall analyse the effects of geometrical and physical parameters of the model and compare these results with experimental data obtained by means of Equation (21). For this purpose we determine $\tau_{\max} = \tau_1(-l/2)$ and

equate it with τ_{ad} and then express τ. Using the notation given in (13) and (18) we obtain

$$\tau_{max} = \tau_1(-l/2) = \tau_2(l/2) = \tau_{ad}$$

$$= \bar{\tau}\left(\frac{V_1 k_0}{k_0 + 2k_1} \text{ th } V_1 + V_2 \text{ cth } V_2\right) - 2(\alpha_1 - \alpha_0)\,\vartheta\,\frac{V_1 \text{ th } V_1}{l(k_0 + 2k_1)} \quad (22)$$

And from (22) we obtain:

$$\bar{\tau} = \frac{P_b}{bl} = \frac{\tau_{ad}(k_0 + 2k_1) + 2(\alpha_1 - \alpha_0)\vartheta V_1(\text{th } V_1)/l}{V_1 k_0 \text{ th } V_1 + V_2(k_0 + 2k_1)\text{cth } V_2} \quad (23)$$

DEPENDENCE OF $\bar{\tau}$ ON GLUE LINE LENGTH

At constant width b = const, V_1 and V_2 in (23) increase linearly with the increase of length; the function of the V_1 increases smoothly from 0 up to 1 while l change from 0 up to ∞. However, at the limit V_2 cth $V_2 = V_2$ th V_2 and at $l \to 0$ is equal to 1. Therefore, the limit of denominator in (23) at $l \to 0$ is equal to $k_0 + 2k_1$, and at $l \to \infty$ it is equal to ∞. The corresponding limits of temperature member are equal to 0. Hence:

$$\lim_{l \to 0} \bar{\tau} = \tau_{ad}, \quad \lim_{b \to \infty} \bar{\tau} = 0 \quad (24)$$

Thus, it follows from (23), that on the glue length change (or glueing area change) from zero up to infinity, the value of quantity $\bar{\tau}$, measured experimentally, should decrease from τ_{ad} up to zero. The last limit means, that beginning from a certain length, the breaking load P_b depends very weakly on the glue length (or area). The graph of showing the dependence of $\bar{\tau}$ on glue length, is given in Figure 7.

Experimental curve 4 of $\bar{\tau}$ dependence on glueing length is presented in Figure 8 which is analogous to theoretical dependence in Figure 7. Experimental curve is obtained with multi-layer specimens like combs, inserted one into another in one plane, their tooth's length changing. In such thin-layer specimens the possible bending of glued glass layers was practically eliminated. Thus, the failure of adhesive joints, resulting from the action of normal breaking stress was prevented.

In Figure 9 (curve 2), the same type of dependence is presented, for the steel substrate and epoxy adhesive.

From the first limit (24) it is possible to estimate the "true" adhesive bond strength of a given adhesive-substrate pair, in complete agreement with its experimentally observed dependence on specimen geometry:

$$\tau_{ad} = \lim_{s \to 0} P_b/S, \quad (25)$$

where S = the glueing area.

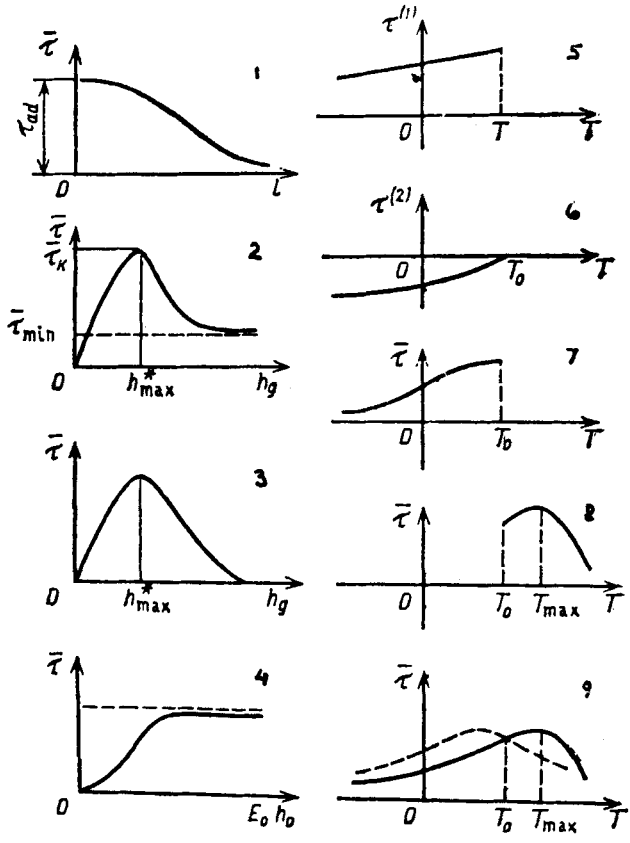

FIGURE 7 Theoretical curves of adhesive strength dependence in shear tests of lap joint on various parameters: 1—on glueing length; 2,3—on adhesive layer thickness; 4—on substrate rigidity; 5–9—on test temperature.

DEPENDENCE OF $\bar{\tau}$ ON ADHESIVE LAYER THICKNESS

The adhesive layer thickness consists of the boundary layer thickness h^* and of the polymer layer thickness h_1, i.e. $h_g = 2h^* + h_1$. Thus, in the beginning, when $h_1 = 0$, the increase of the thickness h_g takes place at the expense of an increase of the boundary layer thickness from zero up to certain limit h^*_{max}. Then h_1 begins to increase from zero up to "infinity." For $h_1 = 0$ the expression (23) assumes the simple form:

$$\bar{\tau} = (\tau_{ad} \cdot \text{th } V_2)/V_2 \tag{26}$$

It follows, that by changing of h^* from zero up to h^*_{max}, the quantity $\bar{\tau}$ increases from zero up to the final quantity $\bar{\tau}_k$, which can be equal to τ_{ad} for low values of

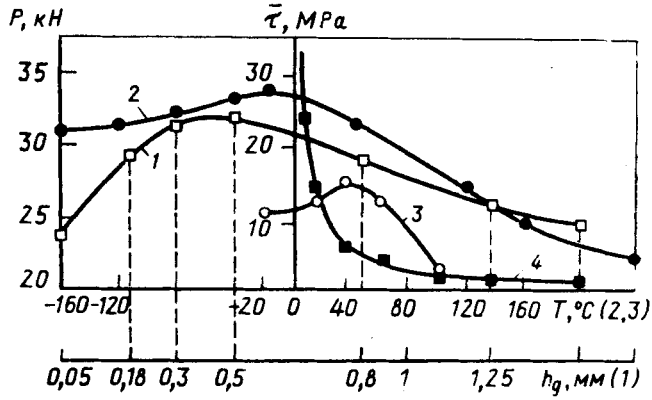

FIGURE 8 Experimental results of shear tests of plate lap joint.

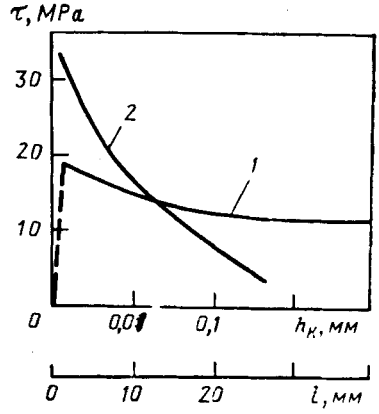

FIGURE 9 Experimental data on dependence of average adhesive strength by lap joint shear steel-epoxy adhesive K-115 on adhesive layer thickness (1) and on glueing length (2).

V_2. Then, while h_1 increases from zero up to "infinity," $\bar{\tau}$ decreases from $\bar{\tau}_k$ to τ_{min} given by

$$\tau_{min} = \frac{k_0 l \tau_{ad} + 2(\alpha_1 - \alpha_0)\vartheta V_2 \text{ th } V_2}{k_0 l V_2(\text{th } V_2 - \text{cth } V_2)} \tag{27}$$

as $k_1 \to 0$ and $V_1 \to V_2$.

If the temperature member in (23), for some value of h_1, is such, that numerator in (23) equals zero, the lower $\bar{\tau}$ limit will represent the zero-model failure resulting solely from temperature stresses, without the application of external force P. Therefore, two types of dependence of $\bar{\tau}$ on h_g are possible as shown in Figure 7.2 and 7.3, of Reference 1.

Figure 8 in which experimental results (curve 1) of dependence on h_g, taken from Reference 2 are given, qualitatively confirms the validity of theoretical conclusions for the example of steel bars glued with filled-in epoxy adhesive "Araldit."

Curve 1 in Figure 9, also shows the experimentally obtained dependence of average shear strength $\bar{\tau}$ of the adhesive joint of steel bars, glued with unfilled-in epoxy resin, on the adhesive layer thickness. Here, we were unable to reach the maximum, at a minimum thickness of 7.6 μm. But we know, that without an adhesive, the adhesive strength will be equal to zero. Therefore, it follows the maximum is at $h^*_{max} \leq 3.8 \times 10^{-5}$ m.

If we neglect the temperature effect in (23), the limit of $\bar{\tau}$ at $h_1 \to \infty$ (27) becomes

$$\bar{\tau}^0_{min} = \frac{\tau_{ad} \text{ th } V_2}{V_2[1 + (\text{th } V_2)^2]}. \tag{28}$$

The square brackets of denominator in (28) have a value which is higher than 1 (but lower than 2). This means, that quantity τ^0_{min} in (28) is lower than $\bar{\tau}$ from (26) by $h^* = h^*_{max}$. It means, that by increasing the adhesive layer thickness h_1 (at constant h^*_{max}) the quantity $\bar{\tau}$ will decrease. Thus, the extremes in $\bar{\tau}$ dependence on h_g can be explained not only by means of temperature (or shrinkage) stresses, but also by considering the boundary layer effects.

$\bar{\tau}$ DEPENDENCE ON SUBSTRATE RIGIDITY

Substrate rigidity $1/k_0 = E_0 h_0$ can be changed either by substrate thickness h_0, or by Young modulus E_0. We assume the other parameters of the model remain unchanged. By increasing $E_0 h_0$ from zero up "infinity," the values V_1 and V_2 change in the range between

$$\infty > V_1 \geq V_1^* = (l/2)\sqrt{2gk_1}, \infty > V_2 \geq 0$$

Using the formula (23) we obtain the possible range of $\bar{\tau}$ by changing $E_0 h_0$ from zero up to infinity:

$$0 \leq \bar{\tau} \leq \tau_{ad} + [(\alpha_1 - \alpha_0)\vartheta V_1^* \text{ th } V_1^*]/k_1 l \tag{29}$$

The change of $\bar{\tau}$ with increase of $E_0 h_0$, obtained from (23) and (29), is given in Figure 7 (curve 4).

The expression (29) indicates the possibility that average adhesive strength $\bar{\tau}$, determined in shear test of lap joint, can be higher than adhesive bond strength τ_{ad} (true strength) of given pair adhesive-substrate. This is very interesting and justifies further investigations.

DEPENDENCE OF $\bar{\tau}$ ON TESTING TEMPERATURE

Considering, that the $V_1 \simeq \text{cth}\ V_2 \simeq 1$, when V_1 and V_2 are sufficiently high. This condition can be easily met by increasing the glueing length l. Consequently we can modify (23) to yield

$$\bar{\tau} = \frac{\tau_{ad}(k_0 + 2k_1)}{k_0 V_1 + (k_0 + 2k_1)V_2} + \frac{2(\alpha_1 - \alpha_0)\vartheta V_1 / l}{k_0 V_1 + (k_0 + 2k_1)V_2}$$

$$= \frac{\tau_{ad}}{(k_0 l/2)\sqrt{g/(k_0 + 2k_1)} + V_2} + \frac{(\alpha_1 - \alpha_0)\vartheta\sqrt{g}}{(k_0 l/2)\sqrt{g} + V_2\sqrt{k_0 + 2k_1}} \quad (30)$$

The model assumes that at a joint manufacturing temperature T_0, and there are no internal stresses. By changing the model temperature from T_0, the elasticity modulus of adhesive E_1 also changes. In Figure 10 the typical curves of Young modulus and of Poisson ratio change of epoxy and polyether polymers determined by acoustic method are presented.[3] To simplify the analysis we assume that the elasticity modulus of substrate E_0 and the rigidity parameter of the boundary layer $g = G/h^*$ do not depend on temperature. We also consider, that the "true" adhesive strength τ_{ad} is independent on temperature.

When the model is "cooled" from the manufacturing temperature T_0, the modulus E_1 increases, as it can be seen in Figure 11. Simultaneously, the parameter k_1 in (30) decreases and so does the parameter V_1. However, V_2 remains unchanged, because it does not depend on k_1 (23). This means, that denominator in the first item $\tau^{(1)}$ in (30) increases slowly with decreasing T, while $\tau^{(1)}$ decreases. The second item $\tau^{(2)}$ in (30), however, will increase with temperature decreasing from T_0. In summary,

$$T \downarrow : E_1 \uparrow,\ K \downarrow,\ \tau^{(1)} \downarrow,\ |\tau^{(2)}| \uparrow,\ \bar{\tau} \downarrow,$$

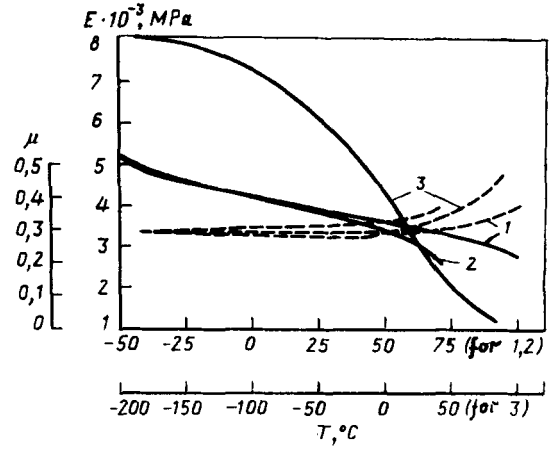

FIGURE 10 Experimental curves of dependence of Young's modulus (full curves) E and of Poisson's ratio (dotted line) of epoxy polymers 6 E-60 (1) 6 EMAP (2) and of polyether resin PN-1 (3). The data from Reference 3.

where arrow on the right shows decreases (downwards) or increases (upwards) of a function or parameter.

In Figure 7, the curves 5–7 present the changes in $\tau^{(1)}$, $\tau^{(2)}$ and $\bar{\tau}$ caused by decreasing temperature. $\bar{\tau}$ quantity, measured in the experiment, should be reduced by temperature decrease from T_0.

When the model is heated above T_0, the maximum of $\tau_1^{(x)}$ (as it follows from 21) will remain for a certain time at $X = -l/2$. In this case, formulas (22), (23) and (30) remain valid. Thus, up to certain temperature $T_{max} > T_0$, τ measured in the experiment continues to grow. But on further increases of T_{exp}, the maximum $\tau_1(x)$ can shift to $x = +l/2$. In this case:

$$\tau_{1max} = \frac{p}{bl}\left(-\frac{V_1 k_0}{k_0 + 2k_1}\,\text{th}\,V_1 + V_2\,\text{cth}\,V_2\right) + \frac{2(\alpha_1 - \alpha_2)\vartheta V_1}{l(k_0 + 2k_1)} \times \text{th}\,V_1 \quad (31)$$

Assuming again that model failure will take place, when τ_{1max} reaches τ_{ad}, it follows that

$$\bar{\tau} = \frac{p_b}{bl} = \frac{\tau_{ad}(k_0 + 2k_1) - [2(\alpha_1 - \alpha_0)\vartheta V_1\,\text{th}\,V_1]/l}{V_2(k_0 + 2k_1)\text{th}\,V_1 - V_1 k_0\,\text{th}\,V_1} \quad (32)$$

And invoking that th $V_1 \simeq$ cth $V_2 \simeq 1$, we obtain

$$\tau = \frac{\tau_{ad}}{V_2[1 - \sqrt{k_0/(k_0 + 2k_1)}} - \frac{(\alpha_1 - \alpha_0)\vartheta\sqrt{g}}{V_2[\sqrt{k_0 + 2k_1} - \sqrt{k_0}]} \quad (33)$$

Both denominators in (33) are positive. With increasing temperature T, the Young modulus decreases, k_1 increases, but k_0 and V_2 remain essentially unchanged. Therefore, the radical in the denominator of the first term decreases while the radical in the denominator of the second term increases. Consequently, the first term slowly decreases with increasing temperature. It can also be deduced from the behavior of the numerator of the second term that it should increase with increasing temperature.

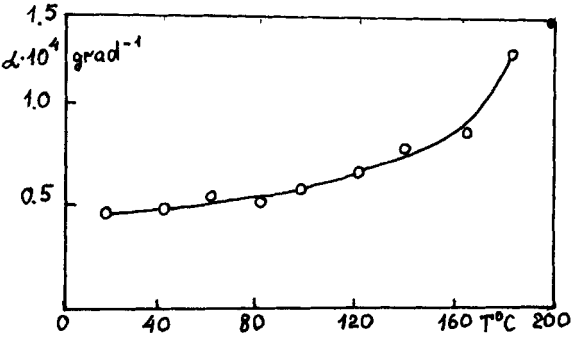

FIGURE 11 Experimental curve of temperature dependence of the coefficient of polyethylene linear expansion.

Since the rate of $\alpha(T)$ increases with increasing temperature (see Figure 11), it follows from (33) that at temperatures above T_0, τ will start decreasing with increasing temperature at a given T_{max}. This is shown in Figure 7 by the solid curve. It should be noted that in this case we considered the failure to be in the boundary layer, namely an "adhesive" failure. We know, however, that the strength of polymeric adhesive is sharply reduced with increasing temperature. This trend leads to the situation where the joint is fractured before τ_{ad} is reached. In this latter case, the model predicts a "cohesive" failure that takes place within the adhesive layer and the maximum of τ on $\tau(T)$ curve will shift to lower temperatures (see Figure 7—the dotted curve).

The experimental data shown in Figure 9 confirm the validity of the theoretical temperature dependence of the lap shear adhesive joint strength ($\bar{\tau}$).

CONCLUSIONS

In conclusion, it should be noted that the computations based on the boundary layer method presented in this study allowed us to explain all the available experimental results of the adhesive lap joint strength, regardless of the fact that we used a one-dimensional approximation.

We have recently used this method to analyze and solve the problems concerning the performance of a number of adhesive joints, both in short- and long-term strength tests. In the latter case, we used non-linear relationship between stresses, deformations and time. Since, the boundary method proved to be very useful in all investigated cases, we are continuing this research to develop models that will cover all steps in the technological process of joint formation to their failure in short- and long-term exposure to external stresses.

LIST OF SYMBOLS

b = width
e = elastic deformation
E = Young modulus
G = shear modulus
h = height of glued plates and adhesive layers
h^* = height of boundary layers
k = one dimensional bar
l = length
N = the force acting upon the units of model width
P = outer (external) forces
sh, ch, th, cth = sinh, cosh, tanh, ctanh
T = temperature
U_k, V_k = components of vector shift of k-plate
W = humidity
x, y = axis

α = coefficient of temperature linear expansion
ϑ = $\Delta T = T - T_0$ – temperature difference
ε^* = viscous-elastic deformations
ε_k^0 = plastic deformations
ε_{th} = temperature strains
ε_{ck} = shrinkage deformations
ε_{hk} = humidity deformations
σ = normal stresses
τ = tangential stresses

Literature

1. R. A. Turusov, A. S. Freidin and V. N. Kestelman, *Intern. J. Polymeric Mater.*, (1995), article in press.
2. B. I. Panshin, in "Adhesives and Glueing Technology," M. Oboronguis, p. 245–259, 1960.
3. A. Ya. Goldman and A. L. Rabinovitch, in "Physical Chemistry and Mechanics of Oriented Glass Plastics," Science, p. 124–129, 1967.